

Mass-scale processing of open-cell metallic foams by pressurized casting method

B. Soni¹ · S. Biswas¹

Published online: 1 July 2016

© Springer Science+Business Media New York 2016

Abstract Here, we report a simple and cost-effective technique for mass-scale processing of open-cell foams of metals and alloys with precise control over foam parameters (pore size, pore distribution, and strut thickness). The process involves pressurized infiltration of molten metals/alloys into salt preforms under 1.5–4 bar inert gas pressure. The preforms were fabricated from spherical particles of different salts, selected on the basis of the melting temperature of the metals/alloys. The porous metallic structures were recovered by leaching out the salt patterns. The working temperature and the applied pressure play the most vital role in determining the foam structure. The developed foams were studied with optical microscope, scanning electron microscope (SEM), and X-ray computed tomography (CT). Mechanical properties of the developed foams evaluated under quasi-static compressive loading are also reported.

Keywords Foam · Infiltration · Casting · Tomography · SEM · Porosity · Strength

1 Introduction

Metallic foams (MFs) have emerged as a new class of engineering materials having number of unique properties such as high gas permeability combined with high thermal conductivity, high compressive strength combined with low density and ultra light weight, striking mechanical

energy absorption characteristics, and higher strength to weight ratios as compared to their bulk counterparts [1–7]. MFs are classified into two types: open-cell and closed-cell foams based on their structure [1, 5]. In closed-cell foams, each cell is completely secluded by a thin wall or crust of the non-permeable metal, whilst in open-cell foams the individual cells are interconnected. Closed-cell foams are generally sought for lightweight structure while open-cell foams are particularly required where surface exchange phenomena are involved or where permeability or pore connectivity is required. In MFs, the ratio of strength per unit mass gets higher with increasing porosity while the quantity of material used decreases. These foams are potentially attractive to be used as high strength and ultra light weight materials in aircrafts, vibration and acoustic energy dampening materials, fluid storage materials, building materials, heat exchangers in power devices, structural materials in space industry, catalyst supports in chemical reactions, porous electrodes, and specifically in high pressure storage systems [1, 8, 9].

Several methods have been explored in manufacturing MFs. The manufacturing processes of MFs can be classified according to the state of matter in which the metals/alloys are processed viz, (i) Liquid state processing, (ii) Solid state processing, (iii) Electro-deposition, and (iv) Vapor phase deposition. Detail reviews of manufacturing methods and characterization of porous metals are available in Refs. [1, 10]. MFs from liquid state can be processed by direct foaming methods, indirect methods via polymer foams, or by casting liquid metal with solid filler materials. Direct foaming of melts by injecting gas for the creation of fine bubbles in the molten metal matrix were carried out in various attempts as described in Refs. [11–13]. The melt was solidified in a controlled manner to trap the gas bubbles during solidification to form the MFs.

✉ S. Biswas
drsomnathbiswas@gmail.com

¹ Department of Physics, The LNM Institute of Information Technology, Jaipur 302031, India

An alternate way of foaming melts is to add blowing agents to the melt instead of blowing gas into it. The reported literature in Refs. [14–18] describes the foaming process of metals using hydrides such as TiH_2 or ZrH_2 as gas forming agents in the molten metal matrix. On heating, the hydrides release hydrogen gas and forms gas bubbles which are trapped inside the molten liquid and form the porous foam structure after solidification. The complete steps involved in processing MFs using hydrides of Ti, Zr, and Hf along with viscosity enhancing agents such as Ca and Mg are described in Refs. [19–21].

Another alternative approach for producing MFs through liquid route is solid–gas eutectic solidification process where a material is melted in a gas atmosphere to saturate it with hydrogen followed by directional solidification at a predetermined pressure causing gas pores to precipitate and getting trapped in the metal [22, 23].

Foams have been manufactured from liquid metal by casting method such as investment casting using polymer foams as starting material and also by direct casting with space holder materials [24–27]. Open-cell polymer foam structure was obtained by reticulation treatment to polyurethane foam followed by filling of heat resistant materials like phenol resin and calcium carbonate or simple plaster [24]. The polymer was removed by heating and then the molten metal was cast into the resulting voids. Removal of the heat resistant material finally created the porous metallic structure. Porous metals were also produced by casting liquid metal around inorganic and organic granules such as soluble salts [28], vermiculite [29], and sand pellets [30] forming syntactic foams which on leaching formed the open-cell structures.

Composite or syntactic MFs were synthesized using pressure infiltration technique [31–36]. High pressure infiltration processes were followed to develop MFs of Al or its alloys [37–43].

Powder compact melting technique was also employed for developing MFs. In this technique, metals or alloys or their blends in powder form is mixed with gas forming/blowing agents which is compacted using hot uniaxial or isostatic compression or by powder rolling followed by heat treatment near the melting point of the metal matrix leading to decomposition of the blowing agent and expansion of the material [44–46]. Some techniques also use a combination of solid and liquid state processing to produce MFs [47]. Modified processes [48–51] have been developed to form MFs by hot compacting the powder mixtures of metal and foaming agent at a temperature where joining of the metal particles takes place primarily by diffusion. Powder metallurgy techniques based on leachable space holder materials were also used for the processing of MFs [52, 53].

Techniques involving deposition of powders on polymer medium were also explored to form MFs. Porous structures of copper and copper alloys were developed by depositing the metals on porous skeletons of resin body by means of an adhesive followed by removing the resin skeleton by heat treatment [54–56]. Electrodeposition process was explored as a convenient technique to fabricate MFs [57–62]. Vapor deposition technique was used to produce MFs of nickel, commercially known as Incofoam [63–65].

Despite of the intense efforts, only few of the currently available MF production methods allow an accurate control over pore geometry and arrangement. While an active research area, there have been very few products that employ MFs. These materials have several perceptible advantages, but the cost of manufacturing good quality foams of both open and closed-cell types has, for the most part, prevented their widespread applications. The present work focuses on the development of a low cost technique for mass-scale production of open-cell MFs with precise control over foam density, shape and size of the pores and their distribution.

2 Experimental

A series of MFs of pure metals and alloys having open-cell structure of controlled pore size and distribution were developed by a relatively simple and cost effective method involving pressurized (1.5–4 bar pressure of Ar) salt infiltration casting process [66]. The present technique is a modified, more facile and more versatile version of the salt replication method proposed by Brothers et al. [67].

The process allows the fabrication of a series of MFs using different preforms of salts. The preform structures were designed as per the requirement of the final morphology in the MFs. The experimental facilities required in manufacturing the porous metals are high temperature-high pressure tube furnace, crucibles (graphite, alumina, zirconia, clay, etc.) of required shape and size, and salts to form the preform structures. Figure 1 presents the primary steps involved in the fabrication of the MFs. The processing details are described below,

Step 1: Easily leachable salt patterns/preforms of different types (as per requirement), from sintered structures to loose particles, and of different materials (NaCl, sugar, sand clay, mixture of NaCl and sand clay, BaF_2 , SrF_2 , etc.) were used in this work. The selection of the preform material was based on the melting temperature and chemical reactivity of the metals/alloys. Few typical examples are given below,

Preform 1: Easily leachable sugar balls coated with sand clay were used as preforms for low melting temperature metals/alloys. The size and number of the spherical balls

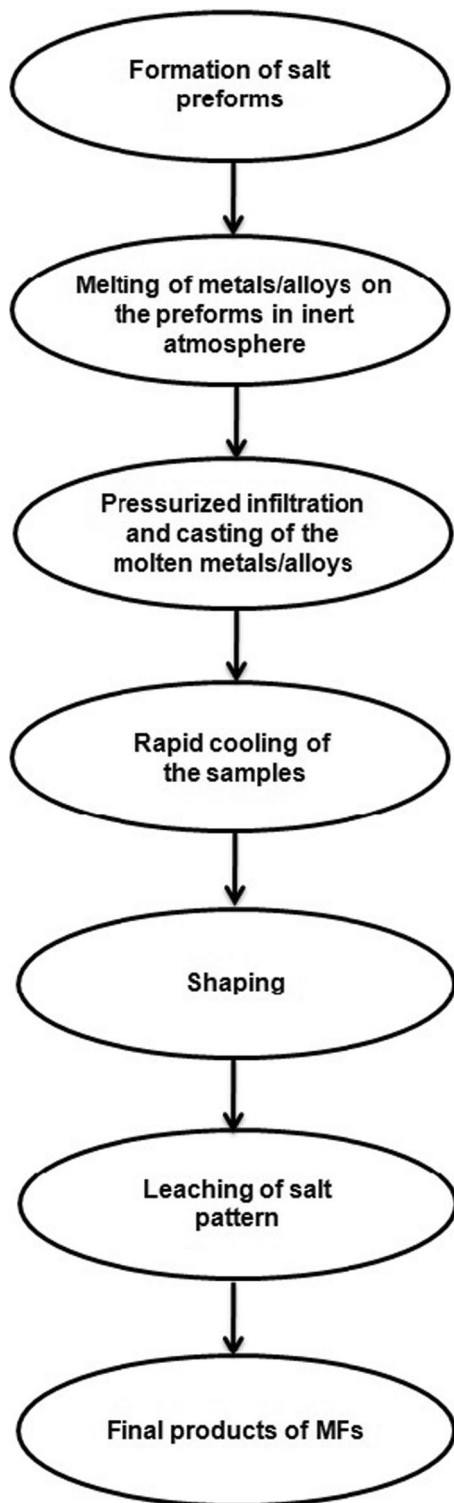


Fig. 1 Flow chart showing the primary steps involved in developing the MFs by pressurized salt infiltration casting process

were selected on the basis of the required pore size and porosity in the final products.

Preform 2: NaCl or clay/sand coated NaCl particles (nearly spherical in shape) were used for alloys with

melting temperature as high as 700 °C. The particles of selected size were sieved and packed in graphite crucibles and heated at 700 °C for 5 h to form the compact preforms.

Preform 3: Preforms of refractory salts were used for high melting temperature metals/alloys. For example, porous patterns of BaF₂ were fabricated from an aqueous slurry of BaF₂ powders (5 μm size particles) and sodium bicarbonate (as foaming agent) in a ratio of 8: 1 (wt%). The slurry was microwave dried to form the porous patterns followed by heating at 850 °C for 5 h in inert atmosphere.

The pressurized infiltration process was carried out in a tube furnace set up as shown in the schematic in Fig. 2. In this process, the casting was performed without any requirement of creating vacuum in the chamber. The preforms were packed in the respective crucibles according to the melting temperature of the metals/alloys. The crucibles are made of graphite, stainless steel, earthen clay, alumina, or zirconia, and are coated with boron nitride to create non sticky surface for the molten metals/alloys. The crucibles have tiny openings/outlets at their basement for gas outflow during the pressurized casting. The dimension of the crucibles was selected in a manner to provide a spontaneous downwards flow of the molten metals/alloys under pressure.

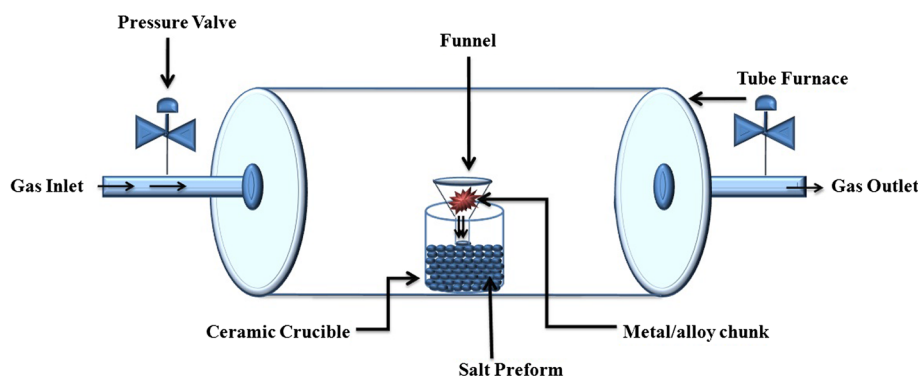
Step 2: The precursor metals/alloys were kept on the preform in the crucible and then placed inside the tube furnace setup having the facility of creating Ar gas pressure up to 4 bar at high temperatures. The metals/alloys were melted at a temperature of 50 °C above their liquidus temperature under continuous flow of inert gas at a pressure of 1.25 bar.

Step 3: The gas pressure was precisely controlled at the inlet and outlet of the furnace chamber to support proper infiltration of the molten metals/alloys into the voids present in the preform. After the pressurized casting, the temperature of the furnace was quickly lowered down at least 50 °C below the solidus temperature of the metals/alloys and the gas pressure was released.

Step 4: The obtained structures were machined into uniform shapes using a diamond grinding wheel and a diamond wafering saw followed by leaching of the salt patterns in hot water or brine solution agitated either by magnetic stirring or ultrasonication followed by pressurized water cleaning wherever required.

Pore distribution in the developed foams was studied with optical microscope, scanning electron microscope (SEM) and computed tomography (CT)-scanner. Cylindrical specimens having dimensions at least 9-times of the average pore size were cut from a parental foam block using electrical discharge machining (EDM) to minimize cell edge damage. The density of the foams (ρ^*) was calculated by measuring the foam volume and mass. The porosity (ϕ) was obtained from the relationship

Fig. 2 Schematic of the tube furnace used for pressurized salt infiltration casting process



$\phi = 1 - \rho^*/\rho_s$ where, ρ_s is density of the solid material from which the foam is made, and the ratio (ρ^*/ρ_s) is termed as the relative density of the foam (ρ_{rel}). Quasi-static compression tests were conducted at room temperature at a strain rate of 0.002 s^{-1} following the ASTM E9-09 standard. At least three specimens were tested for each compressive condition to ensure the reliability of the results.

3 Results and discussion

A series of MFs of pure metals and alloys having open-cell foam structure of controlled shape and size were developed following the present synthesis process involving pressurized salt infiltration casting of molten metals/alloys into the salt preforms placed in ceramic crucibles inside a tube furnace. Figure 3 shows the (a) photographic and (b,c) SEM images of typical open-cell MFs of ASTM B32 grade Sn60 solder alloy (Sn_xPb_y alloy). The pores are almost spherical in shape with a typical diameter of 2–4 mm. Figure 4a, b shows the photographic images of Al foams developed by the present process. The cross sectional view of the Al foam in Fig. 4c elucidates the interconnected open-cell porous structure in the foam. Figure 4d shows the NaCl particles used for forming the preforms. Figure 5a–c shows typical CT-images of the Al foams showing pore dimensions of 1–3 mm ($\phi = 0.50, 0.54$ and 0.62 , respectively). The CT-images clearly reveal the homogeneously distributed interconnected open-cell structure throughout the foam matrix. Figures 3, 4 and 5 confirm that the present process is highly convenient for manufacturing MFs of controlled shape and size along with the required ϕ and pore distributions. Figure 6a shows a typical SEM image of the sintered BaF_2 salt patterns. The porous refractory salt patterns were fabricated from an aqueous slurry of BaF_2 powders ($5 \mu\text{m}$ size particles) and sodium bicarbonate (used as a foaming agent) in a ratio of 8:1 (wt%). The slurry was microwave dried in a controlled manner in a container to form the porous pattern followed by sintering at $850 \text{ }^\circ\text{C}$ for 5 h. Figure 6b shows a typical SEM image of the Al foam structure obtained by

pressurized infiltration of the molten metal in the BaF_2 salt pattern. The salt pattern was leached in a chilled brine solution under continuous sonication and stirring.

The pressurized infiltration of the molten metals/alloys in the salt preforms was accomplished by flushing out the air present in the voids of the preforms placed in the crucible inside the tube furnace. This was achieved by creating the required pressure gradient between the inlet and the outlet of the tube furnace. After melting the metals/alloys under a continuous flow of inert gas, the inlet pressure was quickly increased (and the outlet valve was properly regulated), which essentially forced the molten metals/alloys to infiltrate inside the preform structure. As mentioned before, there are tiny openings at the bottom of the crucibles. These openings allow the passage of the air/gas present in the voids of the preforms when pressure is applied and the voids are subsequently filled with the molten metals/alloys. The spherical salt particles are the most appropriate to be used in forming the preforms, mainly because of two reasons. First, their systematic arrangement in the preforms make the preform structure nearly homogeneous, hence uniform density distribution of the MFs can be achieved. Second, the particles have the least touching surface area in every directions with their nearest neighboring salt particles and thereby provide sufficient void space in the preforms. The spherical shape of the salt particles makes the liquid metals/alloys to flow easily near the touching boundaries of the neighboring particles. When the molten metals/alloys fill the entire void space between the spherical salt particles, they form a metallic cage structure with openings/discontinuities at the positions where the salt particles touch with each other. A moderate gas pressure ensures complete infiltration of the molten metals/alloys in the void space. The required pressure for proper infiltration in the preforms varies with the salt particle size and density of the molten metals/alloys. Higher pressure ($\sim 3\text{--}4$ bar) was required when smaller salt particles ($<750 \mu\text{m}$) were used, while much lower pressure ($1.25\text{--}2.5$ bar) was required when salt particles of larger size ($>1 \text{ mm}$) were used, i.e., higher

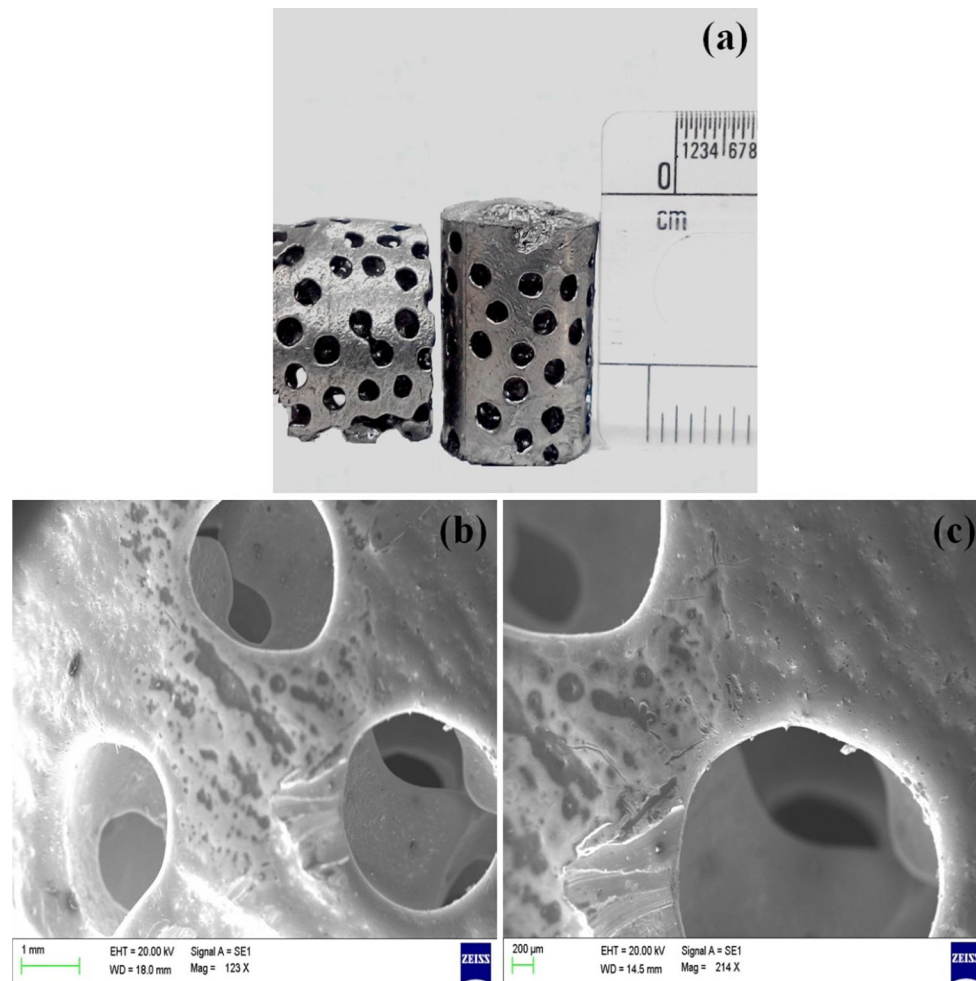


Fig. 3 a Photographic and b, c SEM images of typical MFs of ASTM B32 grade Sn60 solder alloy formed by pressurized salt infiltration casting method

pressure is required for narrower voids. The openings/discontinuities in the metallic cage structure create the interconnected path necessary for the extraction of the solvent during leaching, leaving behind the final structure of the open-cell MFs. Since the entire process of melting, infiltration, and solidification by quenching was performed in inert atmosphere, this process is very useful for those metals having fast reactivity with oxygen and quickly forms oxides on the surface. Several process parameters including the applied gas pressure, working temperature, and the preform structure play vital roles in controlling the foam properties. The molten metals/alloys infiltrated easily at higher temperatures due to the decrease in melt viscosity. For example, molten Al at 680 °C required a gas pressure of 2.5 bar for proper infiltration, while the required pressure decreased to 1.5 bar when the temperature was increased to 720 °C (in both cases salt particles of 1 mm size were used). The ρ_{rel} in both the cases was maintained ~ 0.32 . In the first case, if the pressure is

maintained at 1.5 bar at 680 °C, the ρ_{rel} of the final products decreases to 0.27.

Figure 7 shows the compressive stress versus strain curves under quasi-static loading (strain rate 0.002 s^{-1}) for Al foams with three different relative densities ($\rho_{rel} \approx 0.34, 0.40$ and 0.47 with an average cell size of 2 mm). As can be observed, the curves show the universal compressive characteristics of MFs, i.e., linear elastic response at the beginning of the deformation, an extended plateau region indicating the collapse of the cells followed by final densification stage as the collapsed cells are compacted together and flow stress increases quickly [68].

In metals, sometimes it is difficult to define a yield point at the end of the elastic region on the basis of the shape of stress–strain curve and hence yield point is identified as the point where the curve clearly showed onset of plastic deformation. As can be observed, the samples ($\rho_{rel} \approx 0.34, 0.40$ and 0.47) show very short elastic region under compression with low values of yield strength (σ_y)

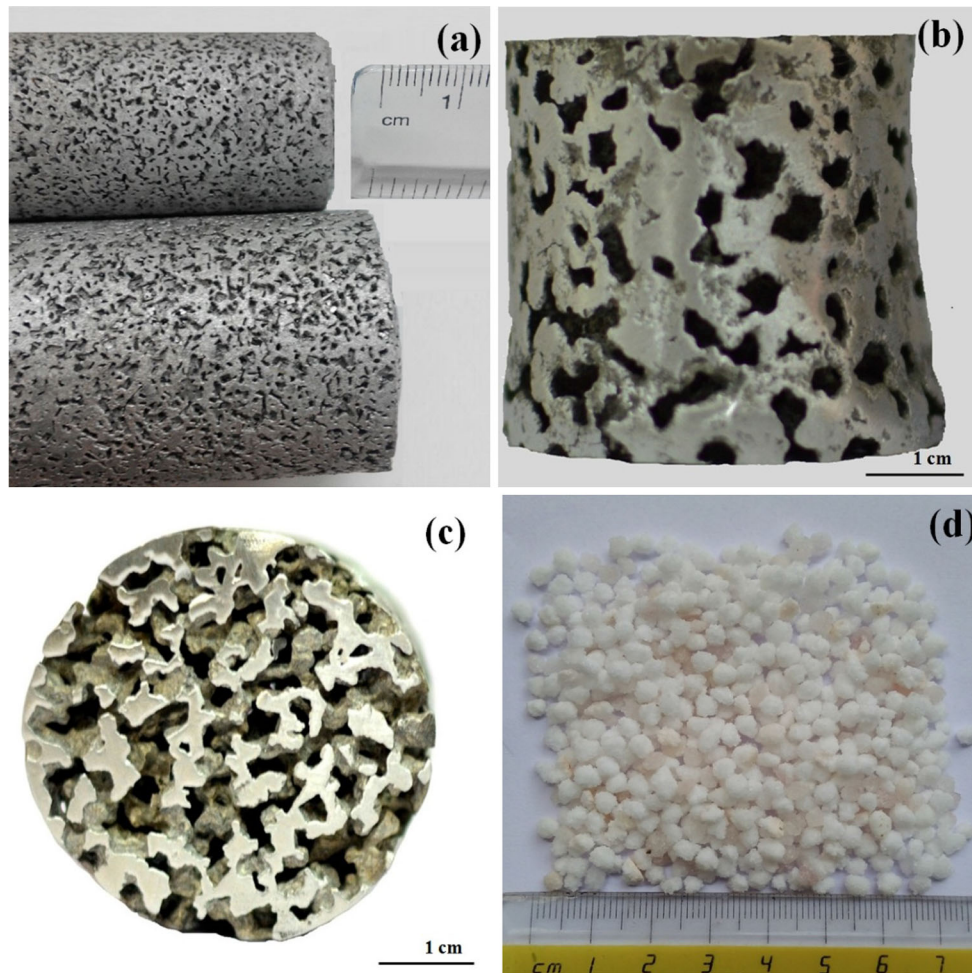


Fig. 4 a–c Photographic images of Al foams formed by pressurized salt infiltration casting method, and **d** the NaCl particles used to form the preforms

(less than 5 MPa), which followed an increasing trend with increasing ρ_{rel} . No clear starting of the rupturing of the first cell band can be clearly visible in any of the curves. Similar behavior of σ_y was also reported by Xiao-qing et al. [69] and Michailidis et al. [70]. The Young's modulus (E) of the three foam samples, as calculated from the slope of the elastic region below the yield point are 141, 199, and 271 MPa, respectively (i.e., E increases with increasing ρ_{rel}). With the increase in ρ_{rel} , the moment of inertia to bend/deform the struts both in elastic and plastic region increases which leads to the enhancement of the compressive properties (σ_y and E) of the MFs. In all the samples, the elastic moduli in the plateau region (E_p) (starting point of plastic region till the onset of densification region) were much smaller than in the elastic region. It confirms that the foams continuously experience bending of the struts and eventually started to collapse after exceeding certain strain level. Such small E_p in MFs is favorable for shock absorption applications.

The ability to absorb mechanical energy during deformation is an important characteristics of MFs. The absorption energy per unit volume (W) and energy absorption efficiency (I) are two important parameters to understand the energy absorption in foams at a specific strain (ε) which can be evaluated by integrating the area under the stress–strain curve and are expressed as [68, 69],

$$W = \int_0^{\varepsilon_m} \sigma(\varepsilon) d\varepsilon \quad (1)$$

$$I = \frac{1}{\sigma_m \varepsilon_m} \int_0^{\varepsilon_m} \sigma(\varepsilon) d\varepsilon \quad (2)$$

where, $\sigma(\varepsilon)$ is the compressive stress (function of ε), ε_m is the limit of plateau strain up to the onset of densification, and σ_m is the corresponding compressive stress. The values of W calculated using Eq. (1) for the above three Al foam samples ($\rho_{rel} \approx 0.34, 0.40$ and 0.47) for an ε_m of 0.4 are 2.2136, 4.9579, and 7.0847 MJm⁻³, respectively. The

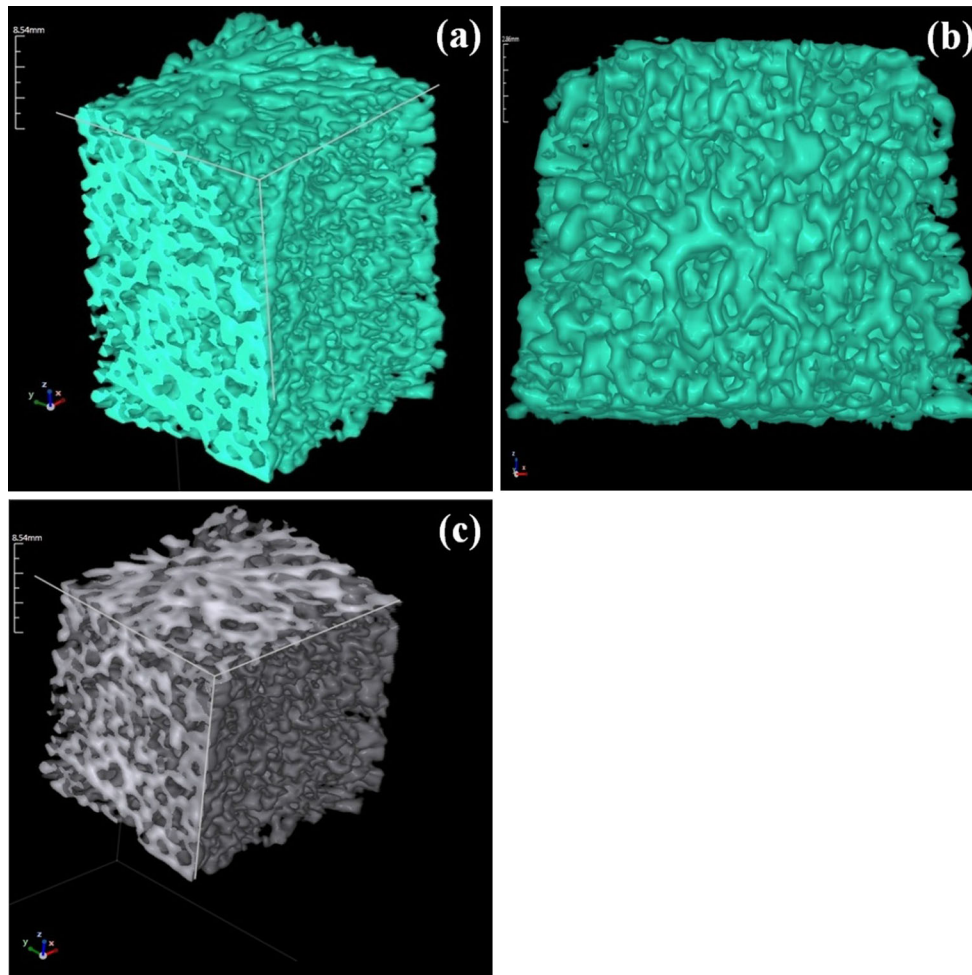


Fig. 5 a–c X-ray tomography generated images of Al MFs ($\phi = 0.50, 0.54$ and 0.62 , respectively)

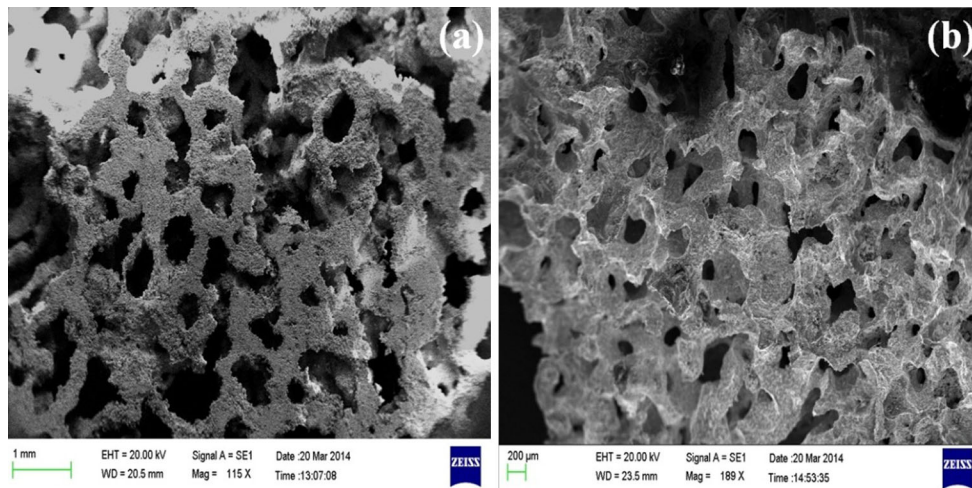


Fig. 6 SEM images of **a** porous BaF_2 salt preform formed by microwave drying of the salt slurry mixed with sodium bicarbonate, and **b** Al MFs obtained after infiltration into the preform

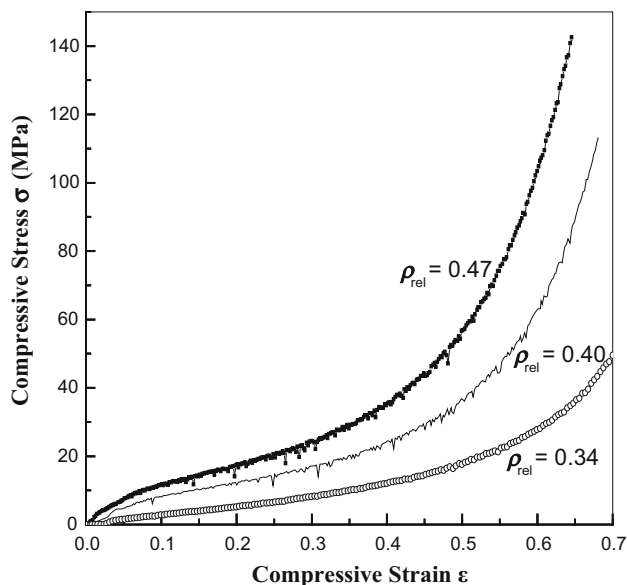


Fig. 7 Compressive stress–strain curves of Al foams of different relative densities ($\rho_{rel} = \rho^*/\rho_s \approx 0.34, 0.40,$ and 0.47) under quasi-static loading (strain rate = 0.002 s^{-1})

corresponding values of I as calculated using Eq. (2) are 46.30, 50.67, and 51.29 %, respectively.

4 Conclusions

A series of MFs of pure metals and alloys with controlled pore size, distribution and strut thickness were derived by pressurized salt infiltration casting process using a high pressure tube furnace and suitable crucibles. The developed process provides a facile way to produce foams of a wide range of metals/alloys for pertinent industrial applications. The process is highly efficient and cost-effective without the necessity of creating vacuum for the infiltration of the molten metals/alloys. Different process parameters affecting the foam morphology were identified and thoroughly studied. It was found that spherical salt particles supports proper infiltration of the molten metals/alloys at 1.5–4 bar pressure. The process can be adopted as an economic and fast technique for mass-scale industrial production of MFs with desired geometries.

Acknowledgments This work has been financially supported by the Department of Science and Technology, Government of India (Project # SR/FTP/PS-214).

References

1. M.F. Ashby, A. Evans, N.A. Fleck, L.J. Gibson, J.W. Hutchinson, H.N.G. Wadley, *Metal Foams: A Design Guide* (Butterworth-Heinemann, Woburn, 2000)

2. C. Körner, R.F. Singer, *Adv. Eng. Mater.* **2**, 159 (2000)
3. J. Banhart, *Prog. Mater. Sci.* **46**, 559 (2001)
4. K.C. Chan, S.H. Chan, *Mater. Manuf. Process.* **19**, 407 (2004)
5. J. Banhart, *Adv. Eng. Mater.* **8**, 781 (2006)
6. L.P. Lefebvre, J. Banhart, D.C. Dunand, *Adv. Eng. Mater.* **10**, 775 (2008)
7. Y.F. Song, L.R. Xiao, X.J. Zhao, H. Zhou, W. Zhang, L. Guo, Y.H. Wang, *Mater. Manuf. Process.* **31**, 1046 (2016)
8. Y. Sugimura, J. Meyer, M.Y. He, H. Bart-Smith, J. Grenstedt, A.G. Evans, *Acta Mater.* **45**, 5245 (1997)
9. H. Nakajima, *Prog. Mater. Sci.* **52**, 1091 (2007)
10. M.F. Ashby, T. Lu, *Sci. China Ser. B Chem.* **46**, 521 (2003)
11. J.A. Ridgeway, US Patent 3297431 (1967)
12. W.W. Ruch, B. Kirkevåg, EP Patent 0483184 (1994)
13. M. Thomas, D. Kenny, H. Sang, CP Patent 2154246 (2004)
14. B. Matijasevic-Lux, J. Banhart, S. Fiechter, O. Görke, N. Wanderka, *Acta Mater.* **54**, 1887 (2006)
15. R.E. Raj, B.S.S. Daniel, *Mater. Manuf. Process.* **22**, 525 (2007)
16. D. Li, J. Li, T. Li, T. Sun, X. Zhang, G. Yao, *Trans. Nonferrous Met. Soc. China* **21**, 346 (2011)
17. Z. Sarajan, M. Soltani, J.K. Khabushan, *Mater. Manuf. Process.* **26**, 1293 (2011)
18. N.V. Anfilov, A.A. Kuznetsov, P.G. Berezhko, A.I. Tarasova, I.A. Tsareva, V.V. Mokrushin, M.V. Tsarev, I.L. Malkov, *J. Alloys Compd.* **645**, S132 (2015)
19. S. Akiyama, H. Ueno, K. Imagawa, A. Kitahara, S. Nagata, K. Morimoto, T. Nishikawa, M. Itoh, US Patent 4713277 (1987)
20. Z. Song, S.R. Nutt, *Mater. Sci. Eng. A* **458**, 108 (2007)
21. K. Morsi, W.M. Daoush, *Scripta Mater.* **105**, 6 (2015)
22. L. Drenchev, J. Sobczak, S. Malinov, W. Sha, *Mater. Sci. Technol.* **22**, 1135 (2006)
23. Y. Liu, Y. Li, J. Wan, *Front. Mech. Eng. China* **2**, 180 (2007)
24. Y. Yamada, K. Shimojima, Y. Sakaguchi, M. Mabuchi, M. Nakamura, T. Asahina, T. Mukai, H. Kanahashi, K. Higashi, *Adv. Eng. Mater.* **2**, 184 (2000)
25. S. Dhara, P. Bhargava, *J. Am. Ceram. Soc.* **86**, 1645 (2003)
26. X.F. Wang, X.F. Wang, X. Wei, F.S. Han, X.L. Wang, *Mater. Sci. Tech.* **27**, 800 (2011)
27. S.F. Fischer, P. Schüler, C. Fleck, A. Bührig-Polaczek, *Acta Mater.* **61**, 5152 (2013)
28. H.A. Kuchek, US Patent 3236706 (1966)
29. J.K. Gibson, J.R. Kreigh, US Patent 3055763 (1962)
30. M.D.I. Zwissler, DE Patent 19725210 (1998)
31. P.K. Rohatgi, R.Q. Guo, H. Iksan, E.J. Borchelt, A. Asthana, *Mater. Sci. Eng. A* **244**, 22 (1998)
32. J.A. Cornie, S.S. Cornie, R.P. Mason, M.A. Ryals, US Patent 6360809 B1 (2002)
33. H.S. Lee, S.H. Hong, *Mater. Sci. Tech.* **19**, 1057 (2003)
34. P.K. Rohatgi, J.K. Kim, N. Gupta, S. Alaraj, A. Daoud, *Compos. Part A Appl. Sci.* **37**, 430 (2006)
35. T.P.D. Rajan, R.M. Pillai, B.C. Pai, K.G. Satyanarayana, P.K. Rohatgi, *Compos. Sci. Technol.* **67**, 3369 (2007)
36. A. Bálint, A. Szlancsik, *Mater. Sci. Forum* **812**, 2 (2015)
37. L. Ma, Z. Song, D. He, *Scripta Mater.* **41**, 785 (1999)
38. J.M. Vihtelic, P.D. Jackson, J.E. Kresta, K.C. Frisch, US Patent 6481490 (2002)
39. L.P. Zhang, Y.Y. Zhao, *J. Compos. Mater.* **41**, 2105 (2007)
40. J.F. Despois, A. Marmottant, L. Salvo, A. Mortensen, *Mater. Sci. Eng. A* **462**, 68 (2007)
41. J.S. Park, S.K. Hyun, S. Suzuki, H. Nakajima, *Metall. Mater. Trans. A* **40**, 406 (2009)
42. A. Jinnapat, A. Kennedy, *Metals* **1**, 49 (2011)
43. J.F. Wang, Y.S. Su, X.L. Gong, *Adv. Mater. Res.* **853**, 125 (2014)
44. J. Baumeister, DE Patent 4018360 (1990)
45. M. Gauthier, L.P. Lefebvre, Y. Thomas, M.N. Bureau, *Mater. Manuf. Process.* **19**, 793 (2004)

46. N. Jha, D.P. Mondal, J.D. Majumdar, A. Badkul, A.K. Jha, A.K. Khare, *Mater. Des.* **47**, 810 (2013)
47. B.C. Allen, M.W. Mote, A.M. Sabroff, US Patent 3087807 (1963)
48. J. Baumeister, H. Schrader, US Patent 5151246 (1992)
49. J. Baumeister, J. Banhart, M. Weber, DE Patent 4426627 (1995)
50. C.J. Yu, H.H. Eifert, J. Banhart, J. Baumeister, *Mater. Res. Innovat.* **2**, 181 (1998)
51. A. Irretier, J. Banhart, *Acta Mater.* **53**, 4903 (2005)
52. G.L. Hao, F.S. Han, W.D. Li, *J. Porous Mat.* **16**, 251 (2009)
53. N. Michailidis, F. Stergioudi, A. Tsouknidas, E. Pavlidou, *Mater. Sci. Eng. A* **528**, 1662 (2010)
54. K. Harada, M. Ishii, K. Watanabe, S. Yamanaka, US Patent 5640669 (1997)
55. C.E. Fanning, US Patent 5759400 (1998)
56. Y. Kamigata, T. Yoshida, K. Susa, T. Uchida, H. Hiratsuka, US Patent 5881353 (1999)
57. W.A. Pruyn, US Patent 5584983 (1997)
58. H.C. Shin, J. Dong, M. Liu, *Adv. Mater.* **15**, 1610 (2003)
59. S. Cherevko, C. Chung, *Electrochem. Commun.* **13**, 16 (2011)
60. N. Ucciardello, S. Guarino, V. Tagliaferri, F. Bertocchi, Patent WO2014141071 A1 (2014)
61. W. Jiang, S.S. Sundarram, W. Li, *Manuf. Lett.* **2**, 118 (2014)
62. B.H. Bui, S. Kim, *J. Electrochem. Soc.* **162**, D15 (2015)
63. J. Babjak, V.A. Ettel, V. Paserin, US Patent 4957543 (1990)
64. D.T. Queheillalt, D.D. Hass, D.J. Sypeck, H.N.G. Wadley, *J. Mater. Res.* **16**, 1028 (2001)
65. <http://www.alloyfoam.com/>
66. S. Biswas, B. Soni, Indian Patent 2015. Application No: 742/DEL/2015
67. A.H. Brothers, R. Scheunemann, J.D. DeFouw, D.C. Dunand, *Scripta Mater.* **52**, 335 (2005)
68. H. Kanahashi, T. Mukai, T.G. Nieh, T. Aizawa, K. Higashi, *Mater. Trans.* **43**, 2548 (2002)
69. C. Xiao-qing, W. Zhi-hua, M.A. Hong-wei, Z. Long-mao, Y. Gui-tong, T. Nonferr, *Metal Soc.* **16**, 351 (2006)
70. N. Michailidis, F. Stergioudi, A. Tsouknidas, E. Pavlidou, *Mater. Sci. Eng. A* **528**, 1662 (2011)